GOSPODARKA SUROWCAMI MINERALNYMI – MINERAL RESOURCES MANAGEMENT

2025 Volume 41 Issue 3 Pages 197–210

DOI: 10.24425/gsm.2025.155340

WOJCIECH WONS[1], KAROL RZEPA[2]

Similarities of Bowen's Reaction Series to the thermal evolution of the siliceous fly ashes phase composition

Introduction

Siliceous fly ash, or class F fly ash (FA), created from the combustion of bituminous coal in conventional boilers, is a fine-grained material with specific grain morphology and phase composition (Vassilev et al. 2004; Blissett and Rowson 2012). It is estimated that over 500 million tonnes of FA are produced annually worldwide (Mathapati et al. 2022). FA grains typically have a spherical shape (Varma et al. 2014; Acar and Atalay 2016), whereas their phase composition is dominated by aluminosilicate glass, mullite, and quartz, which is relatively uncommon in natural rocks. Due to the chemical, phase composition and morphology of FA grains, they are widely used in the building materials industry (Lu et al. 2022), i.a. for the cement and concrete (Canpolat et al. 2004; Komljenović et al. 2009; Juenger and Siddique 2015; Permatasari and Sodri 2023), as well as building ceramics production

✉ Corresponding Author: Wojciech Wons; e-mail: wwons@agh.edu.pl
[1] AGH University of Krakow, Poland; ORCID iD: 0000-0002-0741-6178; e-mail: wwons@agh.edu.pl
[2] AGH University of Krakow, Poland; ORCID iD: 0000-0002-3364-3163; e-mail: krzepa@agh.edu.pl

(Tangsathitkulchai and Austin 1985; Nowok et al. 1993; Ilic et al. 2003; De Casa et al. 2007; Erol et al. 2008; Blissett and Rowson 2012; Acar and Atalay 2013; Eliche-Quesada et al. 2018; Húlan et al. 2020). When analyzing current publications on fly ash, one can notice that their authors do not treat this material as waste, but as a raw material with very interesting properties. Generally speaking, the application goals of these publications focus on the more efficient use of FA. These include publications on the use of FA for the production of geopolymers (Wattimena et al. 2017; Strzałkowska 2021; Król et al. 2024), zeolites (Mlonka-Mędrala 2023; Ibrahim and ElSayed 2021), and the acquisition of microspheres as a thermal insulation material (Krasnyi et al. 2021; Zygmunt-Kowalska et al. 2023). Dudas and Warren presented a model of the FA grain (Dudas and Warren 1987). According to the model, typical FA grain is composed of a glassy matrix with closed gas bubbles in the inner part of the matrix. Small, needle-shaped mullite crystals are embedded in the surface layer of the glass matrix. Small crystals of fly ash minerals are embedded on the surface of the model grain.

However, glassy FA grains are not uniform and vary significantly in density and chemical composition. (Hemmings and Berry 1985; Hemmings et al. 1986; Hemmings and Berry 1987; Qian et al. 1987; Qian and Glasser 1987; Siddique and Khan 2011; Bhatt et al. 2019; Delihowski et al. 2024). According to literature sources, there are the following extreme varieties of the FA glassy phase (Hemmings and Berry 1987):

- Type I glass – low density glass with high SiO_2 to Al_2O_3 ratio content and low modifying oxides content. This type of glass produces thicker, empty inside spherical grains;
- Type II glass – high-density glass with a low SiO_2 to Al_2O_3 ratio and high modifying oxides content. This type of glass creates finer, fuller, and more spherical grains on the inside.

The presence of mullite in FA is the result of the thermal decomposition of kaolinite contained in the gangue. Kaolinite heated to a temperature above 1,100°C undergoes a multi-stage decomposition reaction with mullite as the final product (Allen and Thomas 1999). After the formation of mullite crystals, they grow towards a mostly needle-like form.

Both described features of FA, i.e., a high content of glass dispersed in spherical grains and the presence of mullite, are desirable when used as a component of sintered ceramic mixtures. Hence, FAs are used as raw materials for the production of building ceramics. At temperatures above 900°C, FA undergoes intensive sintering (Nowok et al. 1993). While it is known that mullite, due to the needle-like shape of its grains, improves the mechanical properties of the ceramic body, the influence of glass on the intensification of the sintering process is not fully understood. This article develops this issue and describes the phase composition evolution of FA during heating at various temperatures. Available literature data (Biernacki et al. 2008; Acar and Atalay 2013) indicate that during siliceous FA heating, the amount of mullite increases slightly with a decrease in quartz amount. However, these studies were primarily conducted on coarse-grained FA, in which the influence of the glassy

phase is inconsiderable. The research presented in the article was conducted on fine-grained FA, for which different and more intense effects of phase composition changes were observed.

Furthermore, the finer the FA, the higher its surface energy and therefore the greater the driving force of the sintering process. The separation of fine-grained FA fractions takes place in the electrostatic precipitators, which consist of 3 or 4 sections (zones) arranged in series. Selective collection from the last section of the electrostatic precipitator, located furthest from the boiler, enables the production of fine-grained ashes with a high degree of glass transition (Wons 2010; Małolepszy and Wons 2011). The primary goal of this article is to promote the more effective use of fly ash. In this case, it is used as a raw material for the production of sintered materials, also known as glass ceramics. The authors develop the cognitive goal of determining the thermal conditions and directions of glass crystallization in FA.

1. Materials and methods

The study covered two siliceous FAs from two different Polish power plants, where black coal was burned in pulverized-fuel boilers, and FAs were obtained using electrostatic precipitators. Both FAs came from the section of the electrostatic precipitator furthest from the boiler. Table 1 lists the physical characteristics of FA:

- density determined in an AccuPyc 1330 Micromeritics helium pycnometer;
- specific surface determined by the Blaine method in accordance with PN-EN 196-6:2019-01 (PN-EN 196-6 2019);
- grain distribution determined by the laser method using a Malvern Mastersizer 2000 apparatus in water as a dispersion medium.

Table 1. Physical properties of FA

Tabela 1. Właściwości fizyczne popiołów lotnych

Sample	Physical parameters				
	Density (g/cm^3)	Surface (cm^2/g)	Fraction content (wt.%)		
			(0–20) μm	(20–45) μm	> 45 μm
FA A	2.582 ± 0.003	8,900 ± 100	97.8	2.2	0.0
FA B	2.375 ± 0.002	5,100 ± 100	75.2	16.1	8.7

FA B has a lower density than FA A, because it probably contains a larger proportion of microspheres, i.e., spherical grains filled with gas. Both FAs are not typical, because they are very fine-grained, but FA A is more fine-grained, with 97.8 % of its grains smaller than

20 μm. For comparison, in FA B, 75.2% of grains are smaller than 20 μm. The size of FA grains affects their specific surface area. FA A grains have a much higher surface area than FA B grains.

The chemical composition of FA was determined in accordance with the procedures contained in the standard PN-EN 196-2:2013 (PN-EN 196-2 2013). However, the share of main oxides in the FA was determined by classic titration analysis, while the share of alkali oxides was determined using flame photometry. The analysis for each FA was carried out on two equivalent samples, and the final results presented in Table 2 are the arithmetic mean of two measurements.

Table 2. Chemical composition of FA

Tabela 2. Skład chemiczny popiołów lotnych

Sample	Component content (wt.%)									
	SiO_2	Al_2O_3	Fe_2O_3	CaO	MgO	TiO_2	SO_3	Na_2O	K_2O	LOI
FA A	48.43	28.72	6.35	4.63	2.60	1.17	0.94	1.77	2.81	1.47
FA B	46.40	26.00	9.35	4.90	3.40	1.08	1.93	3.05	2.21	1.06

The phase composition of FA and its sinter was determined by X-ray diffraction (XRD). The radiation source used in this method is an X-ray tube with a copper cathode. The measurement was carried out in the range of 2θ angles from 5° to 60°. Other measurement parameters: number of pulses $10^3 \cdot 2$; lamp intensity 16 mA; tube voltage 35 kV; gap 1°/0.2 mm; counting rate 1°2θ/min; belt feed 1 cm/min; mass constant (Cu) 2.995; step 0.05. In addition to the qualitative analysis of crystalline components, a quantitative analysis was also performed using the Rietveld method, as described by Le Saout et al. (2007). In order to estimate the amorphous phase, repeated XRD/Rietveld tests were carried out on samples mixed with a precisely defined amount of corundum standard. Knowing the percentage of corundum in the sample and the Rietveld analysis result, it is possible to estimate the content

Table 3. Phase composition of FA

Tabela 3. Skład fazowy popiołów lotnych

Sample	Phase content (wt.%)					
	glassy phase	carbon	mullite	β-quartz	hematite	sum
FA A	82.8	1.5	11.6	3.5	0.6	100.0
FA B	82.7	1.1	9.7	6.5	–	100.0

of the amorphous phase. The glassy phase was estimated by assuming that the amorphous phase consists of a glassy phase and an amorphous phase in the form of amorphous carbon. The phase composition of FA is presented in Table 3.

FA consist mainly of aluminosilicate glass and small amounts of mullite and quartz. FA A differs from FA B in a larger amount of glass-forming oxides (SiO_2, Al_2O_3) and a smaller amount of some glass-modifying oxides (Na_2O, CaO, MgO, SO_3). The estimated total amount of glassy phase is at a similar level.

FA are substances that have undergone thermal treatment during coal combustion; however, this does not mean they are thermally inert, as confirmed by subjecting them to thermal analysis using DTA/TG. Thermal differential analysis (DTA) coupled with thermogravimetry (TG) was performed using STA 449F3 Jupiter from Netzsch. The study was conducted in a synthetic air atmosphere at a flow rate of 40 ml/min. The heating rate was 15°C/min. The weight of the samples was 100 mg ± 5 mg. The measurements were combined with gas analysis using EGA (QMS – quadrupole mass spectrometer). Dilatometric tests were conducted using a Bähr-Thermoanalyse GmbH dilatometer. The samples were heated to 1,000°C at a rate of 10°C/min, and after maintaining this temperature for 10 minutes, they were cooled at a rate of 20°C/min. FA dilatometric tests were conducted on cylindrical samples with a diameter of 3 mm and a length of 15 mm, prepared in a laboratory stamp press. FA samples were wet formed in a 5% dextrin solution. The dextrin solution ensures the cohesion of the samples and does not affect their linear changes during heating.

The primary research experiment in this work was the analysis of phase composition changes in the thermal range of exothermic effects, spanning temperatures from 800°C to 1,050°C. The analysis of phase composition changes in FA during sintering was carried out by preparing semi-dry samples from pure FA, subjecting them to thermal treatment at various temperatures, and testing them for quantitative phase analysis using the XRD method. The details of the experiment are included in the diagram in Figure 1. The phase analysis of sinters was performed as for fly ash.

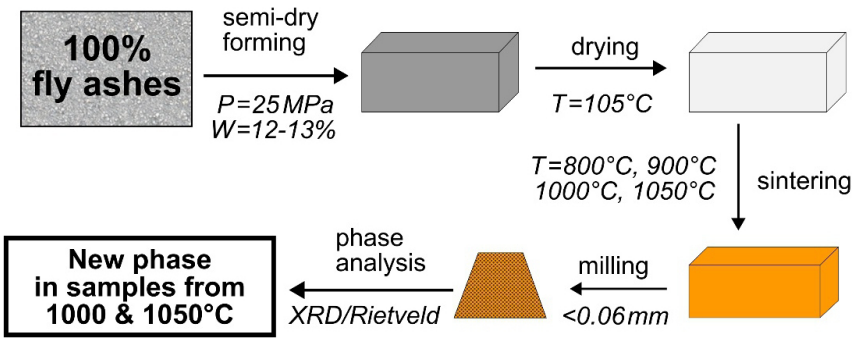

Fig. 1. Scheme of the phase composition evolution research of FA during sintering (Wons 2010)

Rys. 1. Schemat badania ewolucji składu fazowego popiołów lotnych w trakcie ich spiekania

2. Results

The main objective of the DTA/TG thermal tests was to characterize the intensity and temperature range of the exothermic effect associated with the physical and reaction sintering of FA. In traditional FA, this effect begins at a temperature of approximately 850°C to 900°C (Subramanian et al. 2024); however, it is not very intense and is often omitted, or the causes of its occurrence are overlooked. The FA under study exhibits high grain surface development (Table 1), which suggests that the exothermic effect associated with sintering is likely to be intense and may occur at lower temperatures. Figure 2 shows the results of DTA/TG measurements of both FA.

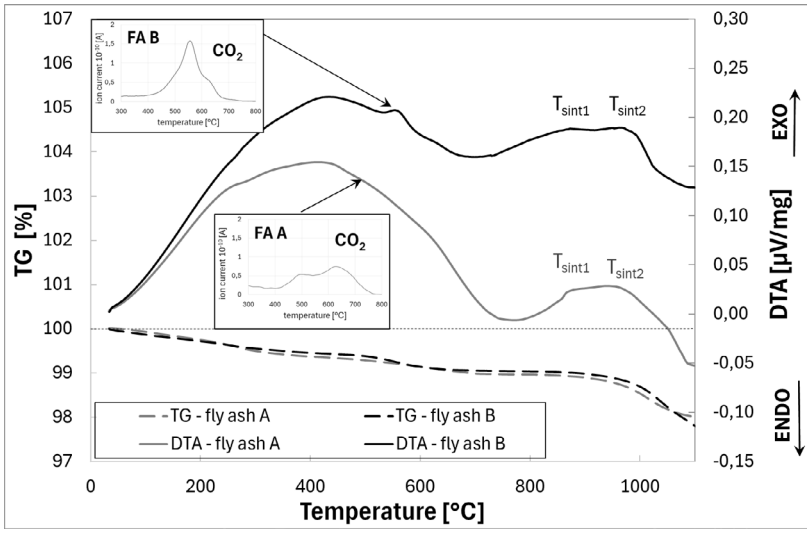

Fig. 2. DTA/TG analysis of FA

Rys. 2. Analiza DTA/TG popiołów lotnych

As can be seen, during the re-thermal processing of FA, there are at least two types of thermal effects. In the temperature range of 400–800°C, the remains of organic substances burn out, as evidenced by the exothermic nature of the effects, the accompanying mass loss, and CO_2 emissions, which occur in conjunction with the effects. The combustion of organic substances in FA is a multi-stage process due to the presence of various types of carbon, such as in hydrocarbons, in the form of graphite or amorphous carbon. The second, strong exothermic effect occurring at temperatures above 750°C (FA B) or above 800°C (FA B) are related to the FA sintering process, as evidenced by the results of dilatometric tests of samples (Figure 3). In both FA, at least two exothermic effects can be observed that

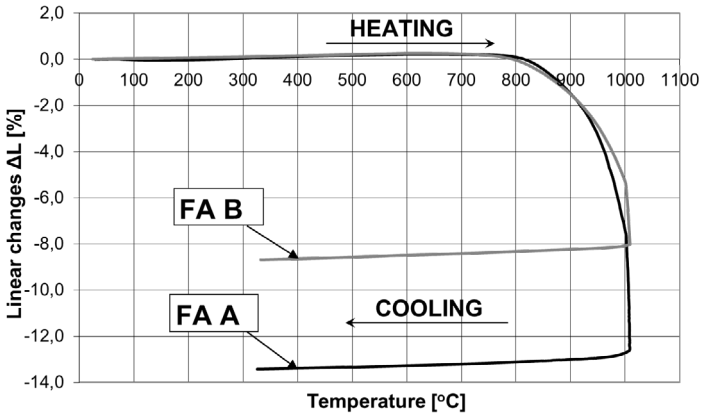

Fig. 3. Linear shrinkage of FA samples

Rys. 3. Skurczliwość liniowa kształtek popiołu lotnego

are superimposed on each other. The extremes of these effects occur at temperatures: for FA A 862°C and 941°C; for FA B 873°C and 963°C.

FA B, despite the similar exothermic effect above temperature 800°C, has significantly lower sintering shrinkage compared to FA A (Figure 3). This led to the hypothesis that other exothermic effects accompany sintering, for example, the synthesis of new phases. To verify this hypothesis, phase analysis of the FA sinter was performed.

Phase analysis of the samples revealed no changes in phase composition in FA sinters up to a temperature of 800°C. In sinters at a temperature of 900°C, small reflections appeared in the diffractograms, but they could not be clearly assigned to specific phases. The amount of these phases was below the detection threshold of the XRD method. In FA sinters at temperatures of 1,000 and 1,050°C, the number of new phases was high enough to be identified and quantitatively analysed. The results of this analysis are presented in Table 4.

Table 4. Phase composition of FA sinters

Tabela 4. Skład fazowy spieków popiołowych

Sample		Phase content (wt.%)							
		glassy phase	carbon	mullite	β-quartz	hematite	plagioclase	olivine	sum
FA A	1,000°C	71.3	–	17.6	–	2.1	1.6	7.4	100
	1,050°C	55.7	–	20.7	1.3	3.1	8.1	11.1	100
FA B	1,000°C	43.4	–	8.9	6.5	4.1	28.8	8.3	100
	1,050°C	42.9	–	14.0	3.7	4.8	26.6	8.1	100

Two completely new phases appeared in the sinter: plagioclase and olivine. The large half-width of these phase reflections in the sintered FA diffractograms indicates that the newly formed phases are very fine-grained. Both components create solid solutions with a wide range of miscibility:

- plagioclase solutions: (albite) $Na[AlSi_3O_8]$ – (anorthite) $Ca[AlSi_2O_8]$,
- olivine solutions: (forsterite) $Mg_2[SiO_4]$ – (fayalite) $Fe_2[SiO_4]$.

The interpretation of the diffractograms shows that the plagioclase formations are rich in anorthite, and the $(Mg,Fe)_2[SiO_4]$ olivines are of the magnesium-iron type. In sinters from FA A and FA B at a temperature of 1,050°C, there is a similar amount of olivines, but in the latter, the content of plagioclases is incomparably higher.

Moreover, during sintering of FA, the amount of mullite and hematite increases, and the quartz present in the ashes practically disappears.

3. Discussion

During the thermal treatment of compressed FA samples, sintering occurs, as evidenced by the physical aspect of shrinkage observed in dilatometric tests. The starting temperature of sintering is similar for both FAs. It is approximately 800°C, while the level of total sintering shrinkage is higher for FA A, which is related to its higher specific surface area (Table 1). During sintering, the development of the grain surface decreases, which is associated with a decrease in surface energy, which indicates the exothermic nature of the process (Lis and Pampuch 2000). The energy released during sintering probably triggers the devitrification process of FA glass at a temperature of approximately 900°C. Initially, based on XRD diffractograms, it was not possible to clearly verify what new phases were formed as a result of glass crystallization, which indicates their fine grain size (cryptocrystallinity) or a low degree of crystallinity in general. At a temperature of 1,000°C, the amount of new phases exceeded the detection threshold by the XRD method. It turned out that, as a result of FA glass partial devitrification, two new products were formed: calcium-rich plagioclase and $(Mg,Fe)_2[SiO_4]$, a magnesium-iron olivine. Interestingly, these are the first two products of the reaction series resulting from the crystallization of basalt magma under deep-sea conditions, i.e., the so-called Bowen Reaction Series (Hamblin and Christiansen 2001). It can be assumed that this analogy of the created products results from the similar chemical composition of FA glass to basalt-type magma. Unlike FA, basalt contains more MgO and CaO, but almost twice as little Al_2O_3 (Dobiszewska and Beycioğlu 2020). These differences in chemical composition are the reason why the analogies of FA glass devitrification to Bowen's Reaction Series end with the newly emerging phases mentioned above. During thermal treatment of FA glass, the amount of mullite is also increased, a phase that is not a characteristic phase of Bowen's Reaction Series or any other Rock Reaction Series. The presence of mullite in the FA and its sinter, which are the subject of the research, results from their creation method and is a kind of genealogical imprint. Mullite grains are formed during

the thermal decomposition of kaolinite, i.e., the phase present in the coal gangue rock from which FA was created. When calcinating FA samples, a maximum temperature of 1,050°C was used. This temperature is lower than the formation temperature of new mullite grains. The increase in the mullite content in FA sinters should therefore be explained only by the growth of existing mullite grains and not by the nucleation of new ones.

Due to the similarity of the substrates (SiO_2 and Al_2O_3), the crystallization of plagioclase and olivine may be partially competitive with the mullite grain growth. Although the SiO_2/Al_2O_3 ratio in the FA is similar, the competitiveness of the reactions may explain the significant differences in the amounts of mullite and plagioclase in FA sinters A and B. In FA B, sinter with a much higher content of plagioclase (over 26%) exhibit an increase in mullite content to a lesser extent (Δ = 4.3%). However, in sinters from FA A containing a smaller amount of plagioclase (8%), a greater increase in mullite content was recorded (Δ = 9.1%). Quantitative differences in the direction of FA glass crystallization result from establishing different mutual equilibria of the new phases. Originally, FA B had a higher content of Na_2O and CaO, i.e., substrates for the formation of plagioclase, which, unlike SiO_2 and Al_2O_3, are not substrates for the formation of mullite. Another interesting but logical aspect of the phase composition evolution of sintered FA samples is the practical disappearance of quartz. As already mentioned, basalt magmas are characterized by a lower Al_2O_3 content than FA, which results in a completely different main oxide components ratio (SiO_2/Al_2O_3). In the tested FA, it was 1.7–1.8, while in basalt magma, it exceeds 3. Hence, there was a significant silica deficiency in the FA glass, which probably caused the "digestion" of the quartz initially present in the FA. During FA heating, the amount of hematite increases, which gives the sinters a characteristic brown-red colour. Hematite is formed either as a result of isolation from the glassy phase or from other iron oxides not detected in XRD tests.

The phase composition evolution of the FA samples can be schematically illustrated as shown in Figure 4.

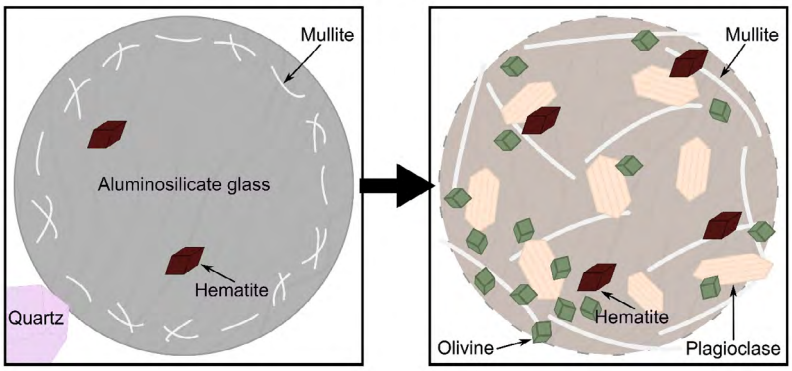

Fig. 4. Evolution of the FA phase composition during thermal treatment

Rys. 4. Ewolucja składu fazowego popiołów lotnych w trakcie obróbki termicznej

According to the proposed scheme, during the thermal treatment of FA at 1,000–1,050°C, the growth of primary mullite grains occurs within their spherical grains, while two new phases appear, which are the products of devitrification of their glass, namely plagioclase and olivine. The quartz grains initially present in the FA gradually disappear, providing substrates for the formation of the aforementioned products, mainly olivine (Figure 4: a higher amount of olivine is observed after thermal treatment within the original quartz grain). The liquid phase is also important for the above-described transformations, as it:

- enables the growth of needle-like mullite crystals,
- etches quartz grains,
- accelerates the transport of substrates to create products.

Conclusions

During the thermal treatment of FA, devitrification occurs, resulting in the formation of products similar to those produced during the first stage of crystallization of basaltic magma in the Bowen Reaction Series, such as olivine and plagioclase rich in CaO. Two other phases were present in the FA before thermal processing: mullite and quartz. While quartz grains gradually disappear, providing substrates for the creation of new products, mullite grains grow. The final phase composition of heat-treated FA sinters depends not only on the thermal treatment conditions (time, temperature, cooling rate) but primarily on the chemical composition, mainly the Na_2O content, the presence of which determines the amount of plagioclase formed. Due to the common substrate effect – Al_2O_3, the increase in plagioclase content limits the growth of mullite grains. An increase in temperature promotes devitrification of the glass unless complete melting occurs. The thermal treatment time is conducive to establishing equilibrium conditions, while the cooling rate influences the level of vitrification of the liquid phase generated during thermal treatment of the ashes.

In summary, the observed FA phase transformations that accompany the sintering process may be important for shaping the parameters of the finished sinter. It is not indifferent whether more mullite or plagioclase is formed in the material during thermal treatment. Mullite enhances the strength of ceramic materials due to the needle-like shape of its grains, and also provides fireproofing and resistance to corrosive factors. However, the crystallization pressure of plagioclase may cause a decrease in the strength of the sintered ceramic material and a decrease in fire resistance.

While the directions of melt crystallization in multicomponent systems are relatively well understood, the directions of devitrification in glasses, even in the presence of crystalline components, are more complex and less well known. The research presented in this paper facilitates the understanding of these mechanisms and indicates that they are not chaotic. By determining the factors influencing the direction of glass crystallization

in FA or other glassy materials, this mechanism can be more easily controlled. The final goal is the effective use of fly ash, taking into account its diversity in terms of chemical composition.

The study was carried out under the statutory work of the AGH University of Krakow no 16.16.160.557.

The Authors have no conflict of interest to declare.

REFERENCES

Acar, I. and Atalay, M.U. 2013. Characterization of sintered class F fly ashes. *Fuel* 106, pp. 195–203, DOI: 10.1016/j.fuel.2012.10.057.

Acar, I. and Atalay, M. U. 2016. Recovery potentials of cenospheres from bituminous coal fly ashes. *Fuel* 180, pp. 97–105, DOI: 10.1016/j.fuel.2016.04.013.

Allen, S.M. and Thomas, E.L. 1999. The structure of materials. New York, DOI: 10.1557/S0883769400053355.

Bhatt et al. 2019 – Bhatt, A., Priyadarshini, S., Mohanakrishnan, A.A., Abri, A., Sattler, M. and Techapaphawit, S. 2019. Physical, chemical, and geotechnical properties of coal fly ash: A global review. *Case Studies in Construction Materials* 11, DOI: 10.1016/j.cscm.2019.e00263.

Biernacki et al. 2008 – Biernacki, J.J., Vazrala, A.K. and Leimer, H.W. 2008. Sintering of a class F fly ash. *Fuel* 87(6), pp. 782–792, DOI: 10.1016/j.fuel.2007.08.024.

Blissett, R.S. and Rowson, N.A. 2012. A review of the multi-component utilisation of coal fly ash. *Fuel* 97, pp. 1–23, DOI: 10.1016/j.fuel.2012.03.024.

Canpolat et al. 2004 – Canpolat, F., Yılmaz, K., Köse, M.M., Sümer, M. and Yurdusev, M.A. 2004. Use of zeolite, coal bottom ash and fly ash as replacement materials in cement production. *Cement and concrete research* 34(5), pp. 731–735, DOI: 10.1016/S0008-8846(03)00063-2.

De Casa et al. 2007 – De Casa, G., Mangialardi, T., Paolini, A.E. and Piga, L. 2007. Physical-mechanical and environmental properties of sintered municipal incinerator fly ash. *Waste management* 27(2), pp. 238–247, DOI: 10.1016/j.wasman.2006.01.011.

Delihowski et al. 2024 – Delihowski, J., Izak, P., Wójcik, Ł., Gajek, M., Kozień, D. and Jarosz, M. 2024. Size fraction characterisation of highly-calcareous and siliceous fly ashes. *Journal of Thermal Analysis and Calorimetry* 149(19), pp. 10587–10603, DOI: 10.1007/s10973-024-13566-x.

Dobiszewska, M. and Beycioğlu, A. 2020. Physical properties and microstructure of concrete with waste basalt powder addition. *Materials* 13(16), DOI: 10.3390/ma13163503.

Dudas, M.J. and Warren, C.J. 1987. Submicroscopic structure and characteristics of intermediate-calcium fly ashes. *MRS Online Proceedings Library (OPL)* 113, DOI: 10.1557/PROC-113-309.

Eliche-Quesada et al. 2018 – Eliche-Quesada, D., Sandalio-Pérez, J.A., Martínez-Martínez, S., Pérez-Villarejo, L. and Sánchez-Soto, P.J. 2018. Investigation of use of coal fly ash in eco-friendly construction materials: fired clay bricks and silica-calcareous non fired bricks. *Ceramics International* 44(4), pp. 4400–4412, DOI: 10.1016/j.ceramint.2017.12.039.

Erol et al. 2008 – Erol, M., Küçükbayrak, S. and Ersoy-Mericboyu, A. 2008. Comparison of the properties of glass, glass-ceramic and ceramic materials produced from coal fly ash. *Journal of Hazardous Materials* 153(1–2), pp. 418–425, DOI: 10.1016/j.jhazmat.2007.08.071.

Gammons et al. 2009 – Gammons, C.H., Harris, L.N., Castro, J.M., Cott, P.A. and Hanna, B.W. 2009. *Creating lakes from open pit mines: processes and considerations, emphasis on northern environments* [Accessed: 2025-05-06].

Hamblin, W.K. and Christiansen, E.H. 2001. *Earth's Dynamic Systems*. Prentice Hall. [Online:] https://books.google.pl/books?id=FRJOAQAAIAAJ [Accessed: 2025-05-06].

Hemmings, R.T. and Berry, E.E. 1985. Speciation in size and density fractionated fly ash. *MRS Online Proceedings Library (OPL)* 65, DOI: 10.1557/PROC-65-91.

Hemmings, R.T. and Berry, E.E. 1987. On the glass in coal fly ashes: recent advances. *MRS Online Proceedings Library (OPL)* 113, DOI: 10.1557/PROC-113-3.

Hemmings et al. 1986 – Hemmings, R.T., Berry, E.E., Cornelius, B.J. and Scheetz, B.E. 1986. Speciation in size and density fractionated fly ash II. Characterization of a low-calcium, high-iron fly ash. *MRS Online Proceedings Library* 86(1), DOI: 10.1557/PROC-86-81.

Húlan et al. 2020 – Húlan, T., Štubňa, I., Ondruška, J. and Trník, A. 2020. The influence of fly ash on mechanical properties of clay-based ceramics. *Minerals* 10(10), DOI: 10.3390/min10100930.

Ibrahim, L.A., and ElSayed, E.E. 2021. Seawater reinforces synthesis of mesoporous and microporous zeolites from Egyptian fly ash for removal ions of cadmium, iron, nickel, and lead from artificially contaminated water. *Egyptian Journal of Chemistry* 64(7), pp. 3801–3816, DOI: 10.21608/ejchem.2021.73834.3661.

Ilic et al. 2003 – Ilic, M., Cheeseman, C., Sollars, C. and Knight, J. 2003. Mineralogy and microstructure of sintered lignite coal fly ash. *Fuel* 82(3), pp. 331–336, DOI: 10.1016/S0016-2361(02)00272-7.

Juenger, M.C.G. and Siddique, R. 2015. Recent advances in understanding the role of supplementary cementitious materials in concrete. *Cement and concrete research* 78, pp. 71–80, DOI: 10.1016/j.cemconres.2015.03.018.

Komljenović et al. 2009 – Komljenović, M., Petrašinović-Stojkanović, L., Baščarević, Z., Jovanović, N. and Rosić, A. 2009. Fly ash as the potential raw mixture component for Portland cement clinker synthesis. *Journal of thermal analysis and calorimetry* 96, pp. 363–368, DOI: 10.1007/s10973-008-8951-0.

Krasnyi et al. 2021 – Krasnyi, B.L., Ikonnikov, K.I., Lemeshev, D.O., Galganova, A.L. and Sizova, A.S. 2021. Investigation of the Possibility of Using Light Aluminosilicate Components of Fly Ash for the Production of Refractory Heat-Insulating Materials. *Glass and Ceramics 78*(7), pp. 323–327, DOI: 10.1007/s10717-021-00403-y.

Król et al. 2024 – Król, M., Stoch, P., Szymczak, P. and Mozgawa, W. 2024. Thermal behavior of coal fly ash geopolymers: structural analysis supported by molecular dynamics and machine learning methods. *Journal of Thermal Analysis and Calorimetry* 149(10), pp. 4397-4409, DOI: 10.1007/s10973-024-13004-y.

Lis, J. and Pampuch, R. 2000. *Sintering* (*Spiekanie*). Kraków: AGH (*in Polish*).

Le Saout et al. 2007 – Le Saout, G., Füllmann, T., Kocaba, V. and Scrivener, K. 2007. Quantitative study of cementitious materials by X-ray diffraction/Rietveld analysis using an external standard. *Proceedings of the 12th International Congress on the Chemistry of Cement, Montréal, QC, Canada*. pp. 8–13.

Lu et al. 2022 – Lu, X., Liu, B., Zhang, Q., Wen, Q., Wang, S., Xiao, K. and Zhang, S. 2022. Recycling of coal fly ash in building materials: a review. *Minerals* 13(1), DOI: 10.3390/min13010025.

Małolepszy, J. and Wons, W. 2011. The influence of the vitreous phase of fly ashes on sintering process. *Materiały Ceramiczne* 63(1), pp. 58–63.

Mathapati et al. 2022 – Mathapati, M., Amate, K., Prasad, C.D., Jayavardhana, M.L. and Raju, T.H. 2022. A review on fly ash utilization. *Materials Today: Proceedings* 50, pp. 1535–1540, DOI: 10.1016/j.matpr.2021.09.106.

Mlonka-Mędrala, A. 2023. Recent findings on fly ash-derived zeolites synthesis and utilization according to the circular economy concept. *Energies* 16(18), DOI: 10.3390/en16186593.

Nowok et al. 1993 – Nowok, J.W., Benson, S.A., Steadman, E.N. and Brekke, D.W. 1993. The effect of surface tension/viscosity ratio of melts on the sintering propensity of amorphous coal ash slags. *Fuel* 72(7), pp. 1055–1061, DOI: 10.1016/0016-2361(93)90308-O.

Permatasari, R. and Sodri, A. 2023. Utilization of Fly Ash Waste in the Cement Industry and its Environmental Impact: A Review. *Jurnal Penelitian Pendidikan IPA* 9(9), pp. 569–579, DOI: 10.29303/jppipa.v9i9.4504.

PN-EN 196-2. 2013. *Cement testing methods – Part 2: Chemical analysis of cement* (*Metody badania cementu – Część 2: Analiza chemiczna cementu*) (*in Polish*).

PN-EN 196-6. 2019. *Methods of testing cement – Part 6: Determination of fineness of grinding* (*Metody badania cementu – Część 6: Oznaczanie stopnia zmielenia*) (*in Polish*).

Qian, J.C. and Glasser, F.P. 1987. Bulk Composition of the Glassy Phase in some Commercial PFA's. *MRS Online Proceedings Library (OPL)* 113, DOI: 10.1557/PROC-113-39.

Qian et al. 1987 – Qian, J.C., Lachowski, E.E. and Glasser, F.P. 1987. Microstructure and chemical variation in class F fly ash glass. *MRS Online Proceedings Library (OPL)* 114, DOI: 10.1557/PROC-114-307.

Siddique, R. and Khan, M. I. 2011. *Supplementary cementing materials*. Springer Science & Business Media, DOI: 10.1007/978-3-642-17866-5.

Strzałkowska, E. 2021. Fly ash – a valuable material for the circular economy. *Gospodarka Surowcami Mineralnymi – Mineral Resources Management* 37(2), DOI: 10.24425/gsm.2021.137563.

Subramanian et al. 2024 – Subramanian, S., Eswar, T. D., Joseph, V. A., Mathew, S. B. and Davis, R. 2024. Fly ash and BOF slag as sustainable precursors for engineered geopolymer composite (EGC) mixes: a strength optimization study. *Arabian Journal for Science and Engineering* 49(4), pp. 5697–5719, DOI: 10.1007/s13369-023-08421-4.

Tangsathitkulchai, M. and Austin, L.G. 1985. Studies of sintering of coal ash relevant to pulverised coal utility boilers: 2. Preliminary studies of compressive strengths of fly ash sinters. *Fuel* 64(1), pp. 86–92, DOI: 10.1016/0016-2361(85)90284-4.

Varma et al. 2014 – Varma, A.K., Kumar, M., Saxena, V.K., Sarkar, A. and Banerjee, S.K. 2014. Petrographic controls on combustion behavior of inertinite rich coal and char and fly ash formation. *Fuel* 128, pp. 199–209, DOI: 10.1016/j.fuel.2014.03.004.

Vassilev et al. 2004 – Vassilev, S.V, Menendez, R., Diaz-Somoano, M. and Martinez-Tarazona, M.R. 2004. Phase-mineral and chemical composition of coal fly ashes as a basis for their multicomponent utilization. 2. Characterization of ceramic cenosphere and salt concentrates. *Fuel* 83(4–5), pp. 585–603, DOI: 10.1016/j.fuel.2003.10.003.

Wattimena et al. 2017 – Wattimena, O.K., Antoni, A. and Hardjito, D. 2017. A review on the effect of fly ash characteristics and their variations on the synthesis of fly ash based geopolymer. *AIP Conference Proceedings*. AIP Publishing, DOI: 10.1063/1.5003524.

Wons, W. 2010. *The influence of silica fly ash properties on the sintering process of ceramic masses* (*Wpływ właściwości krzemionkowych popiołów lotnych na proces spiekania mas ceramicznych*). PhD work, Kraków: AGH (*in Polish*).

Zygmunt-Kowalska et al. 2023 – Zygmunt-Kowalska, B., Zakrzewska, P., Szajding, A., Handke, B. and Kuźnia, M. 2023. Polyurethane foams reinforced with microspheres-assessment of the application in construction as a thermal insulation material. *Thermochimica Acta* 726, DOI: 10.1016/j.tca.2023.179556.

SIMILARITIES OF BOWEN'S REACTION SERIES TO THE THERMAL EVOLUTION OF THE SILICEOUS FLY ASHES PHASE COMPOSITION

Keywords

sintering, devitrification, fly ash, Bowen's Reaction Series, mullite

Abstract

Siliceous fly ashes (FA) are fine-grained thermal decomposition remnants of mineral substances present in bituminous coal. Due to its formation method, FA consists mainly of an aluminosilicate glassy phase, as well as crystalline components, such as mullite and quartz. Formerly treated as waste materials, FAs are now a desirable raw material with numerous applications, particularly in the building materials industry, for instance, as an additive for the production of ceramic building materials. FA suitability in this field of application is determined mainly by its specific impact on the sintering process. The addition of FA to the raw material composition intensifies the firing process, primarily due to the fine grain size and the appearance of a liquid phase during sintering. During the thermal treatment of FA at temperatures above 900°C, in addition to the sintering process, devitrification (or glass crystallization) occurs, resulting in the formation of olivines and calcium-rich plagioclase.

The results presented in this publication demonstrate the formation of calcium-rich plagioclase and $(Mg, Fe)_2[SiO_4]$ olivines of the magnesium-iron type, indicating that the direction of devitrification of FA is similar to the initial stages of basalt magma crystallization, known as the Bowen Reaction Series. This publication aims to explain these similarities. For this purpose, two different FAs were examined for the evolution of their phase composition (XRD) during their heat treatment and thermal properties (DTA/TG, dilatometry).

PODOBIEŃSTWA SZEREGÓW REAKCYJNYCH BOWENA DO TERMICZNEJ EWOLUCJI SKŁADU FAZOWEGO KRZEMIONKOWYCH POPIOŁÓW LOTNYCH

Słowa kluczowe

spiekanie, dewitryfikacja, popiół lotny, szeregi reakcyjne Bowena, mullit

Streszczenie

Popioły lotne krzemionkowe są drobnoziarnistą pozostałością termicznej dekompozycji substancji mineralnych obecnych w węglu kamiennym. Ze względu na sposób powstania popioły składają się głównie z glinokrzemianowej fazy szklistej, jak również składników krystalicznych, takich jak mullit i kwarc. Dawniej traktowane jako odpady, współcześnie popioły lotne są surowcami pożądanymi, z wieloma kierunkami zastosowania, zwłaszcza w przemyśle materiałów budowlanych, między innymi jako dodatek podczas produkcji ceramiki budowlanej. O przydatności popiołów w tym obszarze zastosowań decyduje przede wszystkim ich specyficzny wpływ na proces spiekania. Dodatek popiołów do składu surowcowego intensyfikuje proces wypalania, głównie ze względu na drobnoziarnistość oraz na pojawienie się fazy ciekłej podczas spiekania. Podczas termicznej obróbki popiołów powyżej temperatury 900°C obok procesu spiekania występuje dewitryfikacja (lub krystalizacja szkła), za której sprawą powstają oliwiny i bogate w wapń plagioklazy. Wyniki przedstawione w niniejszej publikacji pokazują powstawanie plagioklazów bogatych w wapń oraz oliwinów typu magnezowo-żelazowego $(Mg,Fe)_2[SiO_4]$, co wskazuje na to, że kierunek dewitryfikacji popiołów jest podobny do początkowych etapów krystalizacji magmy bazaltowej, tzw. szeregów reakcyjnych Bowena. Niniejsza publikacja jest próbą wyjaśnienia tych podobieństw. W tym celu dwa różne popioły lotne zostały przebadane pod kątem ewolucji składu fazowego (XRD) w trakcie ich obróbki cieplnej oraz właściwości termicznych (DTA/TG, dylatometria).